Development and research of basalt plastic material for the flood protection structures

I. G. Lukachevskaya[1*], *A. K.* Kychkin[1], *M. P.* Lebedev[2], *A. A.* Gavrilieva[1], and *A. A.* Kychkin[2]

[1]V.P. Larionov Institute of the Physical-Technical Problems of the North SB RAS, Oktyabrskaya st., 1, 677000 Yakutsk, Russia
[2]Federal Research Center "The Yakut Scientific Center of the Siberian Branch of the Russian Academy of Sciences", Petrovskogo st., 2677000 Yakutsk, Russia

Abstract. Due to the increasing number of catastrophic floods around the world, creation of an effective system to protect against natural disasters became particularly relevant. The paper investigates introduction of the basalt fiber to reinforce the composite sheet piles. Influence of the reinforcing fiber interlacing type on the nature of plastics destruction was established. Results of the work prove that basalt plastic (BP) exhibits higher climatic resistance than the fiberglass plastic (FGP). After post-curing, strength characteristics relative to the second year were decreasing by 15% with BP and by 22% with FGP in extension, and the strength limit in bending was decreasing by 12% with BP and by 47% with FGP. It was experimentally shown that under a long-term stationary thermal and humidity effect of 23°C/68RH, diffusion was observed on the basalt and fiberglass plastics consisting of two stages. The first stage had a satisfactory statistical error and was adequately approximated by the Fick's diffusion model and the relaxation model. The second stage had an unsatisfactory statistical error for approximation and was of the spasmodic nature, while the jump in FGP was the largest indicating that the FGP was more susceptible to destruction exposed to the influence of long-term temperature and humidity regime of 23○C/68 RH, than the BP.

1 Introduction

When constructing various coastline fencing, as well as the hydrotechnical facilities and pits, sheet piles are widely used, which until recently were made mainly of the metal materials. At the same time, wider introduction of the polymer materials plays an important role in technological processes intensification in the construction industry and reducing their metal consumption, decreasing power consumption and labor costs. Polymer composite materials (PCM) set new ways in solving the problems, including the problems of improving the fencing. This is largely due to the fact that their use instead of the traditional materials makes it possible to reduce the weight of products, increase corrosion and chemical resistance without compromising the performance properties.

* Corresponding author: mirkin1611@gmail.com

Main properties of the polymeric materials directly depend on composition of the components, their quantitative ratio and strength of the bond between them. In the Russian and foreign practices, fiberglass (FG) is used as the reinforcing material. FG is economical and therefore most attractive for use in various industries.

However, the use of basalt fibers (BF) as an alternative to the FG was expanding in our country and abroad over the past two decades. In many respects, BF is superior to FG and is comparable in its properties to the carbon fibers (CF). Raw materials base for the BF production is available and practically unlimited. Replacing the existing standard Larsen sheet piles with the basalt plastic composite sheet piles would lead not only to improvement in the physical and mechanical properties, but also to the economic efficiency.

Modern literature on the PCM degradation is studying the influence of various ecological factors on the PCM, including alkaline and acidic solutions [1–3], seawater [2, 4, 5], hydrothermal conditions [6–9], temperature fluctuations [10, 11], UV radiation [12, 13] and elevated temperatures [12, 14]. However, relatively less research was focused on the PCM performance under severe ecological conditions associated with freezing/thawing cycles that simulate climate of the cold regions [15–18].

If at present there is a detailed analysis of alterations in the fiberglass plastics (FGP) mechanical parameters exposed in various climatic regions of the globe, similar detailed studies for the basalt plastics (BP) are missing. Therefore, studying the effects of aging of this composite materials class is required in comparison with the available reliable data on the FGP. Thus, information on the BP climatic resistance is of particular relevance. In this regard, obtaining new information that reveals possibilities of using basalt fiber as the reinforcing material for the composite sheet piles is of significant interest.

2 Experiment methodology and materials

Basalt and fiberglass plastics were used as the samples. They were obtained by infusion, sequential laying of the reinforcing material on the mold, impregnating with the three-component epoxy binder consisting of ED-22, Iso-MTGFA, Agidol 53 cured at the temperature of 160 ±2°C for 4 hours.

1. The 5 mm thick BP sheet consisted of 15 layers of the BP-11/1P-kv-12 basalt fabric and 2 layers (first and last) of the TBC-100P-kv-12. Twill weaving was used. The epoxy binder content in the cured sample was 20±0.5% of the BP weight.
2. The 5 mm thick FGP sheet consisted of 13 layers of the Ortex 560 fiberglass fabric. Linen weaving was used. The epoxy binder content in the cured sample was 13±0.5% of the FGP weight.

In this work, the following materials were used:

– ED-22 epoxy resin, GOST 10587–84;
– Iso-MTGFA hardener, TU 2418-399-05842324-2004, produced by OJSC Sterlitamak Petrochemical Plant;
– Agidol 53 polymerization reaction accelerator, TU 2495–449–05742686–2003, produced by OJSC Sterlitamak Petrochemical Plant.

To determine physical and mechanical properties of the basalt and fiberglass plastics, the obtained samples were subjected to a series of tensile and bending tests using the Zwick Roel Z600 tensile testing machine, type BPC-F0600TN.R09, serial number 160088-2008 (GOST 12004-81) on the basis of the V.P. Larionov Institute of the Physical-Technical Problems of the North SB RAS in Yakutsk. The obtained samples were extended in accordance with GOST 32656–2014 “Polymer composites. Test methods. Tensile test methods”. For tensile testing, samples were prepared in the form of blades with dimensions of 220±0.2×20±0.2×5.5±0.2 with the working area of 60±0.2×10±0.2×5.5±0.2 mm in the amount of 5 pieces for each lot. The loading rate during testing was set at 5 mm/min. An

extensometer was used to register deformation with the accuracy of ±1% over the entire deformation measurement range. Bending tests were carried out by the bending test method according to GOST 25.604-82 “Design calculation and strength testings. Methods of Mechanical testing of Polymeric Composite Materials. Test for Bending Properties at normal, elevated and low temperatures”. 5 samples of BP and FGP were prepared for testing in the form of a rectangular strip with dimensions of 210±0.2×10±0.2×5.5±0.2 mm. The loading rate during testing was set at 5 mm/min.

To test the Charpy impact strength in accordance with GOST 4647-80, samples were prepared with dimensions of 80±0.2×10±0.2×5.5±0.2 mm in 10 pieces of each batch of the plastic samples. Distance between the supports was 40 mm. The tests were carried out on the Amsler RKP-450 instrumented pendulum impact tester produced by Zwick Roell.

The BP and FGP samples open porosity was measured by the hydrostatic weighing. Kerosene was used as the working impregnating liquid due to its high penetrating ability. Samples with dimensions of 80×11×5.5±0.2 mm were preliminarily dried in the ShKV-65(3.5) vacuum drying oven at the temperature of 323 K (50°C) for 5 hours. Weighing in air and in kerosene was carried out on the Sartorius and Vibra Hit analytical balances with the accuracy of 0.0001.

Measurement procedure of the FGP and BP samples was as follows:

- sample weighing (m) in the dry state after drying;
- sample impregnation in kerosene during a day;
- weighing the impregnated sample (m1) in the kerosene;
- weighing the impregnated sample (m2) in the open air.

The fractured samples were examined using the Stemi 2000-C stereoscopic microscope (Carl Zeiss, Germany, 2007) to visually assess the fracture nature.

Microstructure was studied on the JSM-7800F scanning electron microscope (JEOL, Japan) at the low accelerating voltage in the samples bulk.

3 Experiment results and discussion

3.1 Assessment of alterations in physical and mechanical properties during the climatic aging

To assess climatic impact of the extremely cold climate on the plastic mechanical properties of plastics, tensile and bending strength of the original samples and samples after exposure were determined, the data obtained are presented in Table 1. Alteration in the mechanical properties reflects a generalized indicator, i.e. the $k_R=R_t/R_0$ relative conservation coefficient, where R_t takes the limits in tensile strength and bending measured after different exposure times, and R_0 takes the corresponding limits at the initial state.

Table 1. k_R plastic persistence indicator after 2 and 4 exposure years on the open atmospheric stands in Yakutsk

PCM mark	State*	Mechanical indicators, R	Persistence coefficient k_R
BP	K-2	Tensile strength limit	1.04
	K-4		0.89
FGP	K-2		1.11
	K-4		0.89
BP	K-2	Bending strength limit	1.43
	K-4		1.31
FGP	K-2		1.56

	K-4		1.09

Note: *I - initial state, K-2 - after 2 years of exposure, K-4 - after 4 years of exposure

Analysis of the experimental results shows an increase in the plastics mechanical properties after 2 years of exposure on the open stands in Yakutsk. It is known that such an increase in the PCM persistence indicators is due to the polymer matrix post-curing and complies with the results obtained by the other researchers [19-23].

After 4 years of exposure, the tensile strength persistence coefficients for plastics were the same. Values of the strength persistence limit coefficient for the BP samples were by 20% higher than those for the FGP. At the same time, relative to the 2 years exposure, tensile strength characteristics of the BP decreased by 15%, FGP - by 22%, as for the bending strength limit decreased for BP by 12%, for the FGP - by 47%.

3.2 Study of the elastic-strength properties of samples in contact with water

Elastic-strength properties of the BP and FGP samples were studied in the initial state, exposed to contact with sea (model solution, pH=8.22) and river water (Lena River, pH=6.83) at room temperature, as well as after immersion in river water with further freezing (ice water) for 70 days (November 3, 2020 – January 12, 2021).

Figure 1 shows a histogram of the tensile strength limit values of the test specimens.

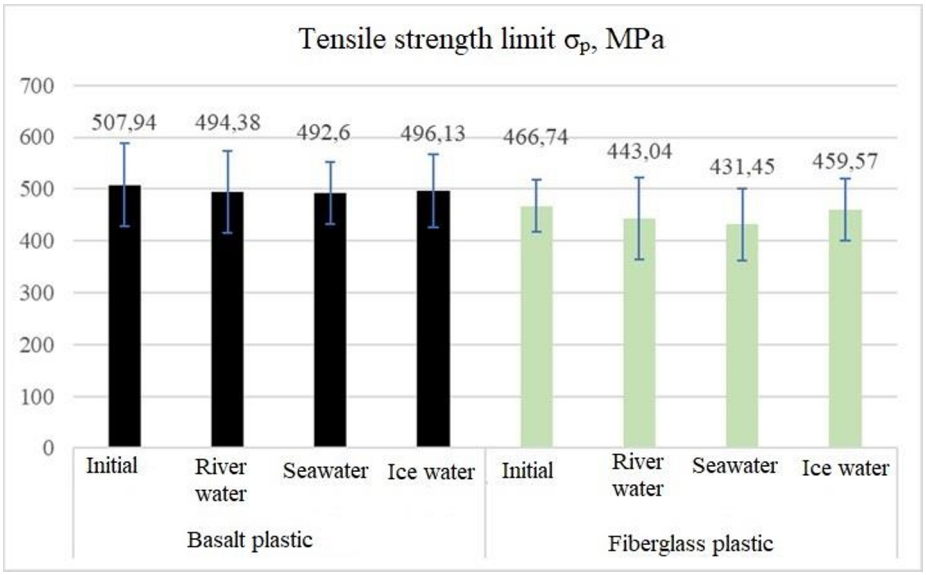

Fig. 1. Samples' tensile testing results

According to the test results, it could be seen that the BP tensile strength values remained practically unchanged in various aqueous media, which could not be noted with the FGP samples. The FGP tensile strength in river water decreased by 5.1%, and in seawater - by 7.6%. However, tensile strength of the specimens exposed in the open air decreased by 2.3% for the BP and by 1.5% for the FGP.

Results of testing plastics for the impact strength by the Charpy method are presented in Figure 2.

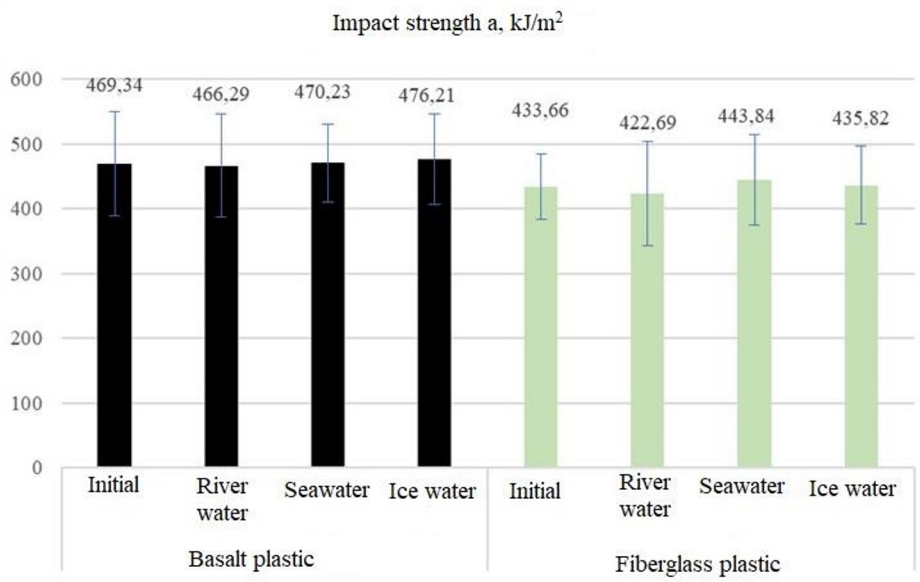

Fig. 2. Samples' impact strength test results

After testing the plastics, it was found that in all samples exposed to the open air the impact strength increased by 1.5% with the BP and by 0.5% with the FGP. Besides, the values of samples in the seawater also increased: BP - 0.2%, FGP - 2.3%.
Study results for the open porosity are presented in Table 2.

Table 2. Open porosity study results (P_o)

Sample	External conditions	Po, %
BP	Initial	0.96 (0. 76….1.19)
	River water	0.76 (0. 55….0.94)
	Seawater	0.88 (0. 82….0.97)
	Ice water	0.81 (0. 68….1.12)
FGP	Initial	0.86 (0. 79….0.93)
	River water	0.68 (0. 55….0.92)
	Seawater	1.10 (0. 87….1.11)
	Ice water	0.89 (0. 81….0.98)

Values of the BP elastic-strength properties in contact with water showed insignificant alterations in contrast to the FGP, where the tensile strength value in river water decreased by 5.1% and in seawater - by 7.6%. Similar jumps were registered in the FGP samples' open porosity values proving the material lower stability in contact with water.

3.3 Investigation of the moisture absorption in basalt and fiberglass plastics exposed to the stationary thermal and moisture influence

The plastics moisture absorption was studied with samples of the original fiberglass and basalt plastics (warehousing) after 24 and 48 months exposure in the Yakutsk conditions. 3 samples were prepared for testing in the form of the 50x50 mm square tiles with a thickness of (5±0.1) mm. in size. There were 18 samples in total. The tests were carried out in a single time interval.

The samples were preliminarily dried in the ShKV-65/3.5 vacuum oven (LLC PF OPTIMUM, Moscow, Russia) at 60°C to the constant weight. The test was carried out in the LABOR MUSZERIPARI MUVEK (ESZTERGOM, Hungary) drying vacuum oven; the samples in the unloaded state were placed in a desiccator over the distilled water with the sulfuric acid solution with the mass fraction of 34% (ρ=1.24944 g/cm^3 at 2 °C) according to GOST 29244–91 and were kept for 100 days. Meanwhile, the samples' masses were periodically measured on the GOSMETR VL-224V analytical balance (LLC Scientific and Production Enterprise Gosmetr, Saint Petersburg, Russia) with accuracy of the fourth decimal, measurement range from 0.00 to 220 g., GOST 9.707–81 accuracy class.

Relative air humidity and temperature inside the desiccator were periodically monitored using the TESTO 623 thermohygrometer with the function trend (error in measuring humidity of ±0.2% and temperature of ±0.2°C, respectively). The device readings were stable during the entire exposure, relative humidity was (68.0±0.2)%, and the air temperature was (23.0±0.2)°C.

Mathematical approximation of the obtained experimental data was performed using the WolframAlpha computational intelligence online program.

Experimental data on the samples' moisture absorption were processed in accordance with GOST 4650–2014. Kinetics of moisture absorption by the sample was determined as the average value of the moisture mass fraction by the samples, M, %, according to the following formula:

$$M = \frac{M_t - M_0}{M_0} \cdot 100 \quad , \qquad (1)$$

where: M_t is the mass of the test sample after soaking (t, days) in moisture, mg; M_0 is the mass of the test sample after initial drying and before immersion in water, mg.

Fig. 3 demonstrates experimental kinetics of moisture absorption by the FGP initial samples and by the FGP samples after the exposure for 24 and 48 months on the open atmospheric stand in Yakutsk. During the first 63 days of moisture saturation, continuous kinetics was observed with a fairly satisfactory static sampling error (Stage 1). After 63 days of moisture saturation, an increase was registered with a jump in moisture content of up to 86 days, then for 4 days it was decreasing to the constant weight (Stage 2). Thus, anomalous diffusion of moisture was observed consisting of two stages.

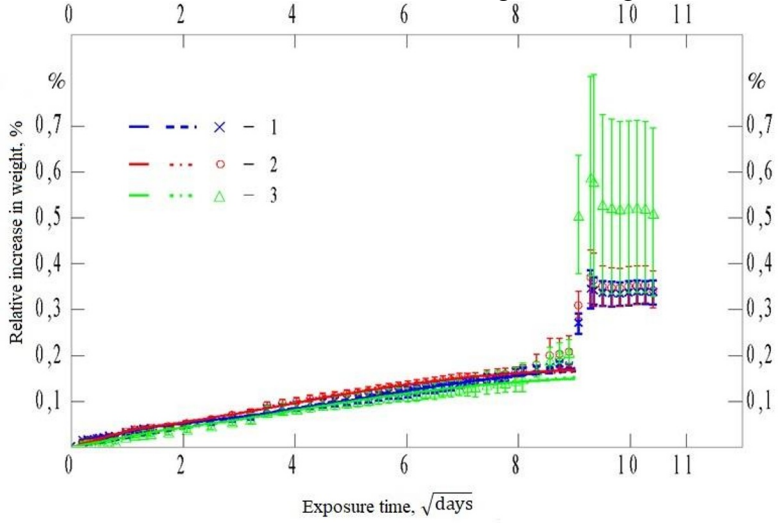

1 - initial; 2 - after exposure for 24 months; 3 - after exposure for 48 months

Fig. 3. Experimental values of moisture content and its approximation (solid line - relaxation model, broken line – Fick's model) in the fiberglass samples

Fig. 4 demonstrates experimental kinetics of moisture absorption by the BP initial samples and by the BP samples after the exposure for 24 and 48 months on the open atmospheric stand in Yakutsk. During the first 80 days of moisture saturation, continuous kinetics was observed with a fairly satisfactory static sampling error (Stage 1). After 80 days of moisture saturation, an increase was registered up to 86 days, then for 4 days it was decreasing to the constant weight (Stage 2). Thus, anomalous diffusion of moisture was observed consisting of two stages.

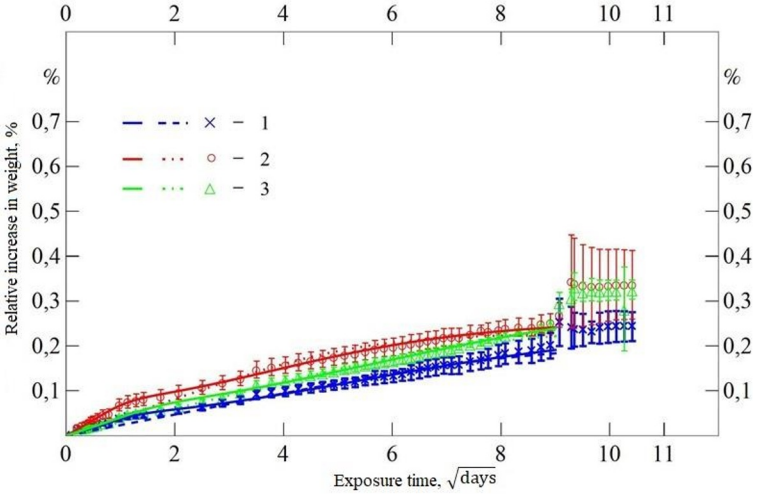

1 - initial; 2 - after exposure for 24 months; 3 - after exposure for 48 months

Fig. 4. Experimental values of moisture content and its approximation (solid line - relaxation model, broken line – Fick's model) in the basalt plastic samples

To approximate the first stage of moisture absorption by the plastics, the abnormal diffusion relaxation model was selected [24, 25]. The relaxation model assumes the variable boundary conditions of the following form:

$$M_\Gamma(t) = M_1 + (M_0 - M_1)e^{-rt},\ r \geq 0, \tag{2}$$

where: M_Γ is the boundary moisture content, %; M_0 is the initial boundary moisture content, %; M_1 is the limiting boundary moisture content, %; r is the relaxation constant, 1/day.

Then, equation for the moisture relaxation sorption kinetics in the infinite plate takes the following form:

$$M_t(t) = M_1 + (M_0 - M_1)e^{-rt} - 8\sum_{k=0}^{\infty} S_k,$$

$$S_k = \frac{\left(M_0 n_k^2 \frac{D}{l^2} - M_1 r\right) e^{-n_k^2 \frac{D}{l^2} t} + r\left(M_1 - M_0\right) e^{-rt}}{n_k^2 \left(n_k^2 \frac{D}{l^2} - r\right)}, \quad (3)$$

where: $n_k = \pi\left(2k+1\right)$; t is the moisture exposure time, days; l is the plate thickness, mm²; D is the Fick's diffusion coefficient, mm²/day.

To determine the D, M_0, M_1, r approximation parameters, the least squares approximation technique was used. In this approach, the squared difference total between the sample experimental and calculated weight gain of

$$\left(\Delta M\right)^2 \equiv \sum_{n=1}^{N} \left(M_{t,n}^{\exp}\left(\%\right) - M_{t,n}^{cal}\left(\%\right)\right)^2 \to \min$$

was minimized by varying the approximation parameters; $M_{t,n}^{\exp}\left(\%\right)$ was the experimentally determined weight of moisture at the t moment of time according to (1); $M_{t,n}^{cal}\left(\%\right)$ was calculated using formula (2); N was the total number of the experimental points. The D, M_0, M_1, r obtained values are presented in Table 3.

Similarly, the Fick's model values (D, $M=M_1=M_0$, $r=0$) were obtained in Table 4. Besides, values of the determination coefficient [25] were also listed.

$$R^2 = 1 - \frac{\left(\Delta M\right)^2}{\sum_{n=1}^{N}\left(M_{t,n}^{\exp}\right)^2 - \sum_{n=1}^{N} M_{t,n}^{\exp} / N}. \quad (4)$$

Formula (4) estimates the share of experimental data described by approximation. If $R^2 = 1$ in formula (4), then the model completely describes the experimental data. The lower adequacy limit according to the Chaddock scale is $R^2 \geq 0{,}81$.

Table 3. Relaxation model approximation parameters

Material	**Exposure term**	***D*, mm²/day**	M_0, %	M_1, %	***r*, 1/day**	R^2
Basalt plastic	Initial	2.75	0.04	0.23	0.018	0.997
	`2 years	3.77	0.08	0.25	0.034	0.997
	4 years	1.63	0.07	0.3	0.016	0.995
Fiberglass plastic	Initial	2.9	0.04	0.21	0.018	0.995
	2 years	4.04	0.04	0.18	0.035	0.992
	4 years	2.3	0.03	0.16	0.032	0.995

Table 4. Approximation parameters by the Fick's model (r=0, $M=M_1=M_0$)

Material	**Exposure term**	***D*, mm²/сут.**	***M*, %**	R^2	M_2, %
Basalt plastic	Initial	0.07	0.2	0.985	0.24
	`2 years	0.16	0.22	0.971	0.34

	4 years	0.08	0.24	0.99	0.33
Fiberglass plastic	Initial	0.06	0.19	0.986	0.26
	2 years	0.1	0.17	0.992	0.35
	4 years	0.07	0.16	0.995	0.52

Determination coefficient calculated values presented in Tables 3 and 4 confirm our assumption that the relaxation model and the Fick's model of moisture absorption describe quite sufficiently moisture diffusion in all the plastic samples under study at the first stage of moisture absorption, and the determination coefficient value was at least 0.971. In this case, the relaxation model had the best determinism coefficient. After that, the limiting moisture content of the second stage appeared abruptly and was defined as the average value of the last seven measurements (Table 3.10). It took 63-80 days to launch the second stage. The maximum average moisture saturation value was 0.5%.

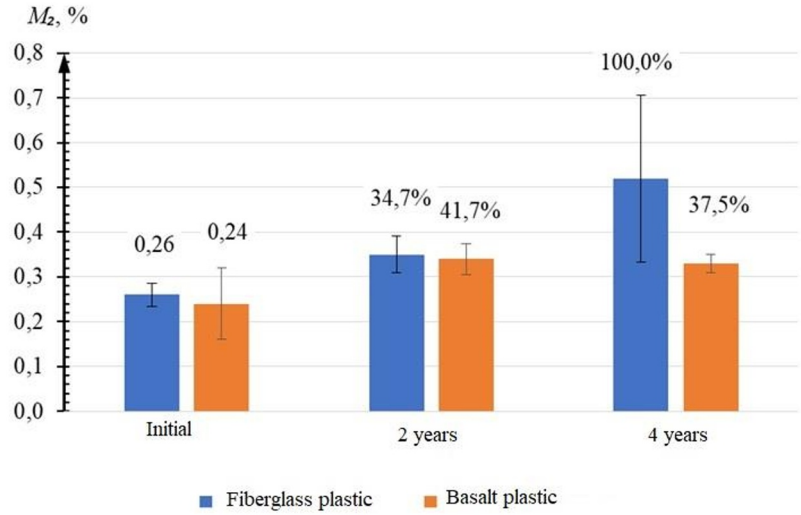

Fig. 5. Limiting moisture saturation of the Stage 2 samples before and after exposure

Figure 5 presents calculated values and growth rates of the limiting moisture saturation of the Stage 2 composites. It could be seen that after the 2 years exposure, the limiting moisture saturation value increased by 34.7% for the fiberglass and by 41.7% for the basalt plastic. And after 4 years of exposure it increased by 100% for the fiberglass and by 37.5% for the basalt plastic, which indicated that the FGP was subjected to greater destruction under the influence of the long-term thermal and moisture regime of 23°C/68 RH, than the BP.

4 Conclusions

1. Retention coefficients of the samples' mechanical properties increased after the 2 years exposure on the open stands in Yakutsk, the city characterized by the extremely cold climate (k_R BP=1.11, k_R FGP=1.22). After 4 years of exposure, the limiting tensile strength retention coefficients for plastics were the same, the values of the limiting strength retention coefficient for the BP samples were by 20% higher than those for the FGP.

2. The decrease in the FGP strength characteristics was more noticeable. Relative to the second year, the BP tensile strength characteristics decreased by 15%, the FGP - by 22%. The bending strength for the BP was decreasing by 12%, for the FGP - by 47%. After the 2 years exposure, the limiting moisture saturation value increased by 34.7% with fiberglass and by 41.7% with the basalt plastic, and after the 4 years exposure it increased by 100% with fiberglass and by 37.5% with the basalt plastic.
3. After staying in water with different pH for 70 days, the BP samples' strength characteristics underwent minor changes, in contrast to the FGP, where the tensile strength value in the river water decreased by 5.1% and in the seawater - by 7.6%.
4. Limiting moisture saturation is a sensitive indicator of the PCM sample macro-damages. Experimental kinetics of the moisture absorption by original and exposed plastics in the cold climate of Yakutsk has two stages of moisture absorption at the long-term thermal and humidity regime of 23°C/68 RH for 108 days. The Fick's and the relaxation models are adequately approximating the first stage (63-80 days), while the relaxation model has the best determinism coefficient. After quasi-equilibrium of the first stage, an increase is observed in the second stage with a jump in the moisture content of up to 86 days, then within 4 days it decreases to the constant weight. At the same time, the maximum average value of moisture saturation for the FGP is 0.56% and 0.42% for the BP. The diffusion coefficient indicators of the BP samples had the linear growth pattern with close values equal to 2-3 mm2/day, while the FGP after 48 months of exposure showed a significant increase in the diffusion coefficient of up to 12 mm2/day, compared to 4-4.5 mm2/day with the control samples and the samples after exposure for 24 months. This is confirmed by the open porosity and average surface heterogeneity data, according to which FGP after 48 months showed a higher degree of surface destruction.
5. Limiting moisture saturation is a sensitive indicator of the PCM sample macro-damages. Experimental kinetics of the moisture absorption by original and exposed plastics in the cold climate of Yakutsk has two stages of moisture absorption at the long-term thermal and humidity regime of 23°C/68 RH for 108 days. The Fick's and the relaxation models are adequately approximating the first stage (63-80 days), while the relaxation model has the best determinism coefficient. After quasi-equilibrium of the first stage, an increase is observed in the second stage with a jump in the moisture content of up to 86 days, then within 4 days it decreases to the constant weight. At the same time, the maximum average value of moisture saturation for the FGP is 0.52% and 0.34% for the BP.
6. Control of the deformation-strength characteristics in combination with the moisture transfer method makes it possible to identify patterns in physicochemical transformations in the polymer volume, determine the level of reversible and irreversible alterations in the control parameters and draw a conclusion on the climatic resistance of epoxy compositions under study. The obtained work results prove that basalt plastics are exhibiting higher climatic resistance.

The work was carried out within the framework of State Assignments of the Ministry of Science and Higher Education of the Russian Federation (No. 122011400350-7 and No. 121032200039-9) and Grant No. 13.TsKP.21.0016.

References

1. M. Bazli, H. Ashrafi, A. V. Oskouei, Effect of harsh environments on mechanical properties of GFRP pultruded profiles. Compos. Part B Eng., **99**, 203–215 (2016)
2. X. Wang, L. Jiang, H. Shen, Z. Wu, Long-Term Performance of Pultruded Basalt Fiber Reinforced Polymer Profiles under Acidic Conditions. J. Mater. Civ. Eng., **30**, 04018096 (2018)

3. Z. Wang, X.-L. Zhao, G. Xian, G. Wu, R. S. Raman, S. Al-Saadi, A. Haque, Long-term durability of basalt-and glass-fibre reinforced polymer (BFRP/GFRP) bars in seawater and sea sand concrete environment. Constr. Build. Mater., **139**, 467–489 (2017)
4. L. Yan, N. Chouw, Effect of water, seawater and alkaline solution ageing on mechanical properties of flax fabricepoxy composites used for civil engineering applications. Constr. Build. Mater., 99, 118–127 (2015)
5. Z. Lu, J. Xie, H. Zhang, J. Li, Long-term durability of basalt fiber-reinforced polymer (BFRP) sheets and the epoxy resin matrix under a wet–dry cyclic condition in a chloride-containing environment. Polymers, 9, 652 (2017)
6. H. Xin, A. Mosallam, Y. Liu, C. Wang, Y. Zhang, Impact of hydrothermal aging on rotational behavior of web-flange junctions of structural pultruded composite members for bridge applications. Compos. Part B Eng., **110**, 279–297 (2017)
7. H. Xin, A. Mosallam, Y. Liu, F. Yang, Y. Zhang, Hydrothermal aging effects on shear behavior of pultruded FRP composite web-flange junctions in bridge application. Compos. Part B Eng., **110**, 213–228 (2017)
8. Z. Wang, G. Xian, X.-L. Zhao, Effects of hydrothermal aging on carbon fiber/epoxy composites with different interfacial bonding strength. Constr. Build. Mater., **161**, 634–648 (2018)
9. B. Hong, G. Xian, H. Li, Comparative study of the durability behaviors of epoxy-and polyurethane-based CFRP plates subjected to the combined effects of sustained bending and water/seawater immersion. Polymers, **9**, 603 (2017)
10. P. K. Dutta, D. Hui, Low-temperature and freeze-thaw durability of thick composites. Compos. Part B Eng, **27**, 371–379 (1996)
11. J. M. Sousa, J. R. Correia, S. Cabral-Fonseca, A. C. Diogo, Effects of thermal cycles on the mechanical response of pultruded GFRP profiles used in civil engineering applications. Compos. Struct., **116**, 720–731 (2014)
12. H. Ashrafi, M. Bazli, A. Vatani Oskouei, L. Bazli, Effect of sequential exposure to UV radiation and water vapor condensation and extreme temperatures on the mechanical properties of GFRP bars. J. Compos. Constr., **22**, 04017047 (2017)
13. M. M. Shokrieh, A. Bayat, Effects of ultraviolet radiation on mechanical properties of glass/polyester composites. J. Compos. Mater., **41**, 2443–2455 (2007)
14. M. Bazli, H. Ashrafi, A. Jafari, X.-L. Zhao, H. Gholipour, A. V. Oskouei, Effect of thickness and reinforcement configuration on flexural and impact behaviour of GFRP laminates after exposure to elevated temperatures. Compos. Part B Eng., **157**, 76–99 (2019)
15. M. Di Ludovico, F. Piscitelli, A. Prota, M. Lavorgna, G. Mensitieri, G. Manfredi, Improved mechanical properties of CFRP laminates at elevated temperatures and freeze–thaw cycling. Constr. Build. Mater., **31**, 273–283 (2012)
16. J. Sousa, J. Correia, J. Gonilha, S. Cabral-Fonseca, J. Firmo, T. Keller, Durability of adhesively bonded joints between pultruded GFRP adherents under hydrothermal and natural ageing. Compos. Part B Eng., **158**, 475–488 (2019)
17. S. A. Grammatikos, R. G. Jones, M. Evernden, J. R. Correia, Thermal cycling effects on the durability of a pultruded GFRP material for off-shore civil engineering structures. Compos. Struct., **153**, 297–310 (2016)

18. A. Jafari, H. Ashrafi, M. Bazli, T. Ozbakkaloglu, Effect of thermal cycles on mechanical response of pultruded glass fiber reinforced polymer profiles of different geometries. Compos. Struct., **223**, 110959 (2019)
19. O. V. Startsev, M. P. Lebedev, A. K. Kychkin, Aging of polymer composites in extremely cold climates. Izvestiya Altayskogo gosudarstvennogo universiteta - Izvestiya of Altai State University, **1(111)**, 41–51 (2020)
20. E. N. Kablov, E. N. Startsev, Systematical analysis of the climatic influence on mechanical properties of the polymer composite materials based on domestic and foreign sources (review). Aviatsionnye materialy i tekhnologii – Aviation materials and technologies, **2**, 47–58 (2018)
21. E. N. Kablov, O. V. Startsev, A. S. Krotov, V. N. Kirillov, Climatic aging aviation applications of composite materials. I. Mechanisms of aging. Deformatsiya i razrushenie materialov – Deformation and Fracture of Materials, 11, 19–26 (2010)
22. E. N. Kablov, O. V. Startsev, A. S. Krotov, V. N. Kirillov, Climatic aging aviation applications of composite materials. II. Relaxation of the initial disequilibrium and structural properties of the gradient across the thickness. Deformatsiya i razrushenie materialov – Deformation and Fracture of Materials, **12**, 40–46 (2010)
23. E. N. Kablov, O. V. Startsev, A. S. Krotov, V. N. Kirillov. Klimaticheskoe starenie kompozitsionnykh materialov aviatsionnogo naznacheniya. III. Znachimye faktory stareniya [Climatic aging aviation applications of composite materials. III. Significant factors of aging]. Deformatsiya i razrushenie materialov – Deformation and Fracture of Materials, **1**, 34–40 (2011)
24. A. L. Pomerantsev, Methods of nonlinear regressive analysis for simulating kinetics of the chemical and physical processes, d-r fiz.-mat. nauk – Diss Dr. Sci. (Phys.-Math.), Moscow, 304 (2003)
25. O. V. Startsev, A. S. Krotov, Sorption and diffusion of moisture in the fiberglass rods of circular cross section. Materialovedenie – Material Science, 6, 24–28 (2012)